

2D and 3D MHD Simulations of Disk Accretion by Rotating Magnetized Stars: Search for Variability

Marina M. Romanova

Akshay Kulkarni, Min Long, Richard V.E. Lovelace, Justin V. Wick

Dept. of Astronomy, Cornell University, Ithaca, NY

Galina V. Ustyugova, Alexander V. Koldoba

*Keldysh Institute of Applied Mathematics and Institute of Mathematical Modeling,
Russian Academy of Sciences, Moscow*

Abstract

We performed 2D and full 3D magnetohydrodynamic simulations of disk accretion to a rotating star with an aligned or misaligned dipole magnetic field. We investigated the rotational equilibrium state and derived from simulations the ratio between two main frequencies: the spin frequency of the star and the orbital frequency at the inner radius of the disk. In 3D simulations we observed different features related to the non-axisymmetry of the magnetospheric flow. These features may be responsible for high-frequency quasi-periodic oscillations (QPOs). Variability at much lower frequencies may be connected with restructuring of the magnetic flux threading the inner regions of the disk. Such variability is specifically strong at the propeller stage of evolution.

Key words: Accretion disks, magnetized stars, dipole field, X-ray, variability

1 Rotational Equilibrium State and Two Main Frequencies

We first investigated slow viscous disk accretion to a rotating star with a dipole magnetic field in axisymmetric (2.5D) numerical simulations. Quiescent initial conditions were developed so that we were able to observe the accretion for a long time [1]. These simulations have shown that many predictions of the theories developed in the 1970's (e.g., [2]–[4]) are correct. Namely, we observed that (1) the accreting matter is stopped by the magnetosphere at the

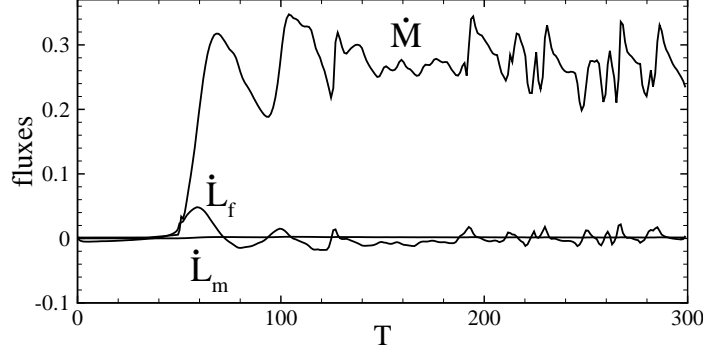


Fig. 1. Fluxes in the rotational equilibrium state. \dot{M} is the matter flux, \dot{L}_f is the angular momentum flux associated with the field (it varies in time but is zero on an average), and \dot{L}_m is an angular momentum flux associated with matter (it is about 100 times smaller than \dot{L}_f).

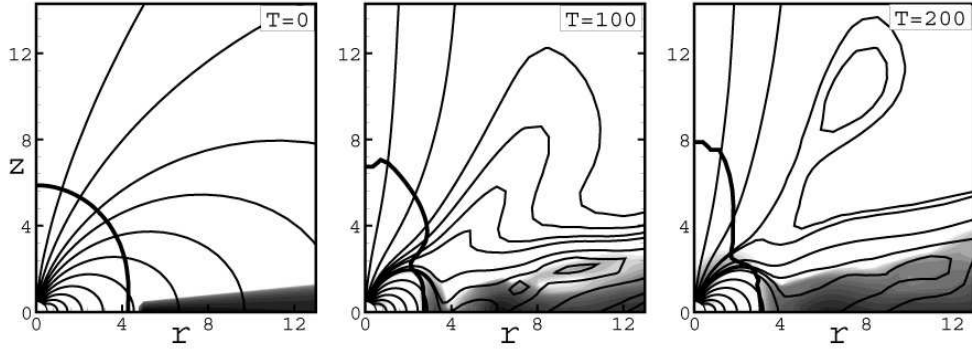


Fig. 2. Density distribution (background), magnetic field lines (thin lines) and the $\beta = 1$ line (thick line) where the matter ram pressure equals the magnetic pressure.

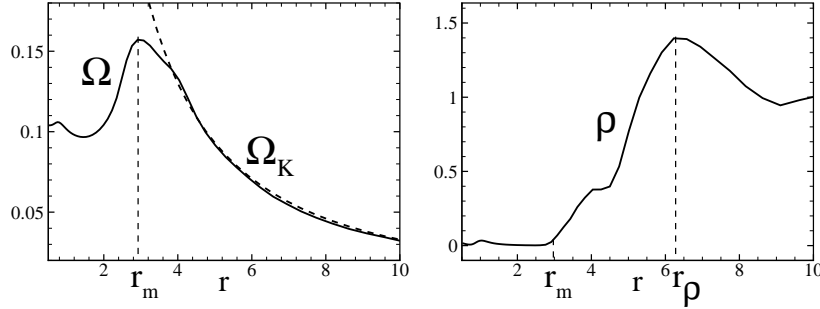


Fig. 3. *Left panel:* Radial distribution of the angular velocity in the equatorial plane. The dashed line shows the Keplerian velocity. *Right panel:* Density distribution.

magnetospheric radius r_m , where the ram pressure $\rho v^2 + p$ equals to magnetic pressure $B^2/8\pi$, and is then lifted up and accretes to the star through funnel flows; (2) the magnetosphere influences the structure of the disk to a distance $r_\Psi \approx (2-4)r_m$; (3) a star may spin-up, spin-down, or may be in the *rotational equilibrium state* depending on the ratio between magnetospheric radius r_m and corotation radius $r_{co} = (GM/\Omega_*^2)^{1/3}$, as predicted by Ghosh and Lamb

[3], [4]. We searched for the rotational equilibrium state and investigated this state in detail [5]. Namely, we fixed the parameters of the disk and magnetic moment of the star, and changed the angular velocity of the star, Ω_* . We found angular velocity Ω_{eq} at which the angular momentum flux to the star is zero on an average. Figure 1 shows the variation of fluxes at the surface of the star for the run with $r_{co} = 5$: the matter flux \dot{M} and the angular momentum fluxes \dot{L}_m and \dot{L}_f associated with the matter and the magnetic field respectively. The flux \dot{L}_f (which always dominates over \dot{L}_m) varies but is approximately zero on an average. We found that in the rotational equilibrium state $r_{co}/r_m \approx 1.4 - 1.7$. Figure 2 shows an example of matter flow in the rotational equilibrium state. We see that matter accretes to the star through a funnel flow, and that some field lines are closed and others are inflated or radially stretched by the accreting matter. Part of the magnetosphere, however, is always closed or only partially open, and this interaction is important for the spin-up/spin-down of the star. The fluxes in Figure 1 vary with time because of inflation and reconnection events in the magnetosphere. We observed that in the rotational equilibrium state the rotation of the star is locked at some value $\Omega_{eq} \approx k\Omega_m$, where $k \approx (1.4 - 1.6)$ and Ω_m is angular velocity of the disk at the magnetospheric radius. The number k is smaller (larger) at smaller (larger) magnetic moments of the star μ . These two frequencies, $\nu_* = (2\pi)^{-1}\Omega_*$ and $\nu_m = (2\pi)^{-1}\Omega_m$ may represent two fundamental frequencies in each binary system in the equilibrium state. Figure 3 (left panel) shows that for our typical case, shown in Figure 2, this ratio $\nu_m : \nu_* \approx 3 : 2$ (see Figure 3, left panel). This ratio is reminiscent of the typical ratio between the frequencies of the kHz QPOs observed from many LMXBs [6],[7]. The surface of the star may be “marked” by hot spots associated with accretion or thermonuclear burning at the surface of the star, while the inner disk radius, which is approximately equal to magnetospheric radius r_m , may be marked by enhanced density in the disk or with enhanced reconnection at the boundary between magnetosphere and the disk. Matter often accumulates and forms a larger density peak or, ring, at the radius $r_{ring} \approx r_m$, thus giving a “mark” to this region. However, in some cases, the density peak is located at larger distances, as is shown in Figure 3 (right panel). The position of this peak varies with the accretion rate. It is closer to r_m during periods of enhanced accretion. In case of accretion to a misaligned dipole the ring typically breaks into two spiral arms (see next section) which rotate with the frequency of the inner regions of the disk.

2 3D Simulations and High-frequency QPOs

We performed full three-dimensional simulations of the disk-magnetosphere interaction [8],[10],[11], for aligned angular momenta of the star and the disk,

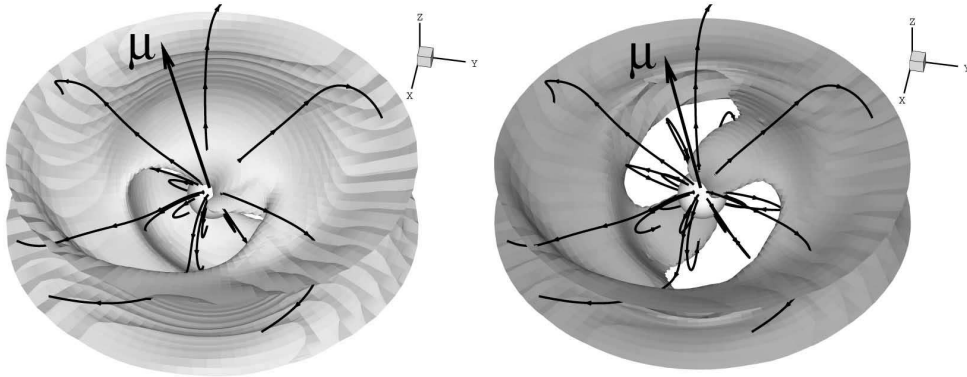


Fig. 4. Magnetospheric flow is different at different density levels: matter blankets the entire magnetosphere at $\rho = 0.2$ (left panel), but forms the funnel streams at $\rho = 0.4$ (right panel). The $\Theta = 30^\circ$ case is shown.

and for different misalignment angles Θ between the magnetic and rotational axes. We observed that many features of the interaction are similar to those in the axisymmetric case. However, in the 3D case, many new features appear which are connected with the non-axisymmetry of the flow and which are important for analysis of high-frequency QPOs.

Simulations have shown that matter typically accretes in two streams. In cases of relatively high-temperature of the disk [11] or non-stationary accretion, more than two streams may form. The shape of the magnetospheric flow strongly depends on the density. In the same simulation run we see that the largest density matter flows in narrow streams, while the lower density matter may blanket the magnetosphere completely (see Figure 4). So variability may be related to radiation/obscuration by the magnetospheric streams. The frequency of this quasi-periodic variability will be between $\nu \sim \nu_*$ and the frequency of the inner region of the disk, ν_m , which is higher than ν_* in the rotational equilibrium state (see Section 1), but may be lower in some other cases. If two or several funnel streams form, then the frequency will be twice or several times higher than that expected in case of one stream.

Other features which may lead to quasi-periodic oscillations are non-axisymmetric features observed in the inner regions of the disk. Matter typically forms two-armed spiral waves which may contribute to quasi-periodic variability (see example in Figure 5). The frequency associated with these features is $\nu_{spirals} \lesssim 2\nu_m$. We should note that in case of the dipole field there are always two features, from opposite sides of the accretion disk, so that the frequency is twice as the frequency of the disk.

Significant variability and quasi-periodic variability may be associated with the *spots* at the surface of the star. The shape of the spots, and also distributions of density, velocity, matter and energy fluxes, reflect those in the funnel

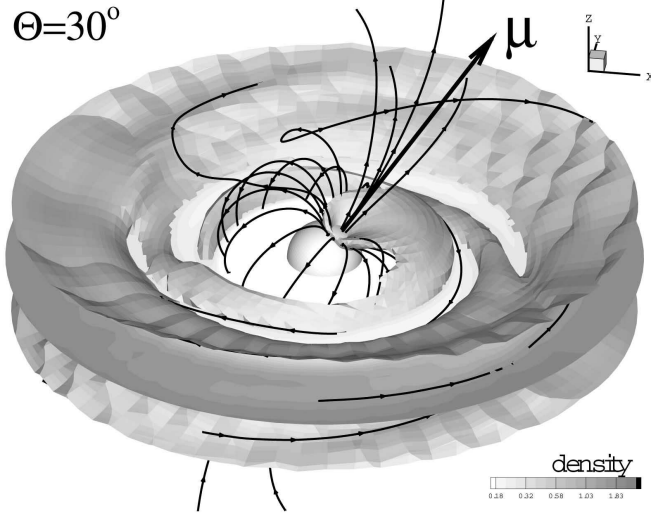


Fig. 5. Example of magnetospheric flow observed in 3D simulations for $\Theta = 30^\circ$. Inner regions of the disk form a trailing spiral structure.

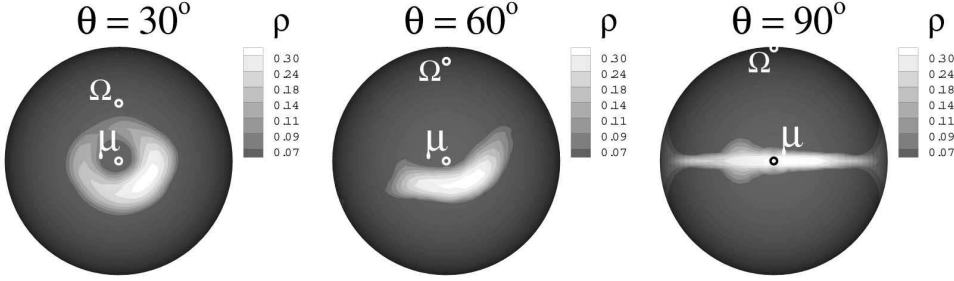


Fig. 6. Density distribution in the hot spots at the surface of the star for different Θ in the relativistic case (from [12]).

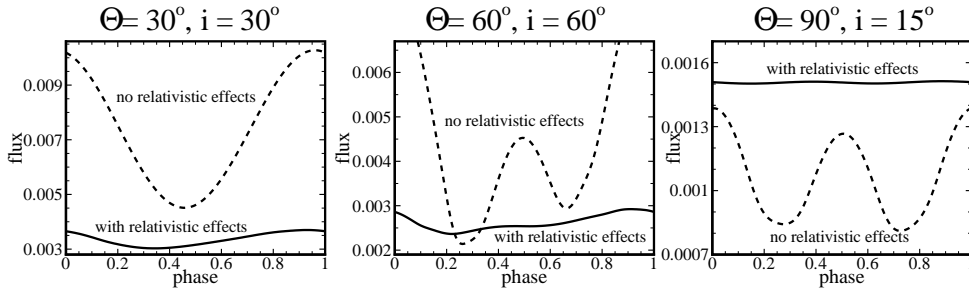


Fig. 7. Examples of variability curves with relativistic effects (solid lines) and without relativistic effects (dashed lines) at different Θ and inclination angles i (from [12]).

streams: at small misalignment angles $\Theta < 30^\circ$, the spots have the shape of a bow, while at large misalignment angles $\Theta > 75^\circ$, they have the shape of an elongated bar [8],[12] (see also Figure 6). It is a common belief that the hot spots have fixed positions at the surface of the star. Simulations have shown

that the positions of the spots vary with time. If the disk is relatively cold, or the misalignment angle is large ($\geq 45^\circ$), then the spots change their shape and position only slightly, so that their frequency slightly varies around stellar frequency $\nu \sim \nu_*$. However, if the disk is relatively hot and the misalignment angle is small ($\leq 30^\circ$), then the funnel streams and spots may rotate faster or slower than the star, because one of foot-points is dragged by the disk, which may rotate faster or slower than the star. This may lead to significant departure of the associated frequency ν_{spot} from the ν_* . The expected frequency ν_{spot} is in between ν_* and ν_m . Temporary events of precession of the funnel streams (and spots) are expected in periods of non-stationary accretion.

The light curves from the hot spots are different for different misalignment angles Θ and inclination angles i . To investigate these dependencies, we fixed hot spots at the surface of the star at some moment corresponding to quasi-equilibrium, and then investigated light curves for different Θ and i assuming that all kinetic energy of the flow is converted to black-body radiation [8]. We observed that the amplitude of variability may be quite large and either one or two peaks can be observed depending on Θ and i . Typically, two peaks are observed at larger Θ and i . However, in accretion to neutron stars, general relativistic, Doppler, and other effects are important (e.g., [13],[14]). Typically, the GR effect dominates unless the star rotates extremely fast. We performed 3D simulations taking into account GR effects (approximated by the Paczyński-Wiita potential) and other effects for neutron stars with parameters close to those in millisecond pulsars. We observed that the shapes of the spots are very similar to those in the non-relativistic case [12] (see Figure 6). We also observed that light bending effects strongly decrease the amplitude of the variability curves [12] (see Figure 7), agreeing with earlier predictions (see, e.g. [15]). In extreme cases, like $\Theta = 90^\circ$ and $i = 15^\circ$, both spots are observed at the same time, so that the amplitude of variability becomes very small (Figure 7, right panel; see also [15]).

These two main features associated with (1) spots at the star and (2) spirals at the inner radius of the disk may lead to high-frequency quasi-periodic oscillations. Simulations have shown that in case of the dipole magnetic field there will be *two symmetric features* (two spirals and two hot spots) and this will double the frequency. We should note that there is another important frequency, a beat frequency: $\nu_b = \nu_m - \nu_*$ which is taken into account in the Beat-Frequency and related models (see [16], [17]). This frequency will correspond to the lower frequency oscillations. If magnetic field of the star is dynamically unimportant then the Sonic-Point model may be applicable for analysis of QPOs ([18]). However we did not model cases with such a weak magnetic field.

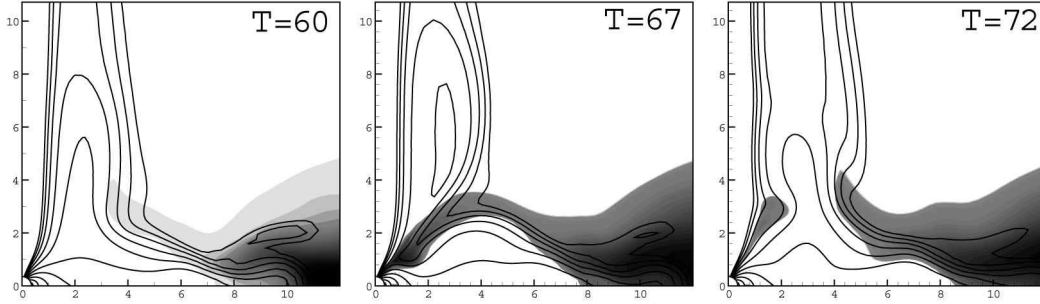


Fig. 8. Example of accretion at the weak propeller stage: matter accumulates and accretes quasi-periodically to the star, forcing magnetic field lines in the magnetic “tower” to reconnect (from [24]).

3 “Propeller” Stage and Low-frequency QPOs

Simulations often show variability of fluxes at much longer time-scales (see, e.g., figure 1). This variability is connected with restructuring of the external magnetic field lines in the corona as a result of the disk-magnetosphere interaction. Such variability appears at different rotation rates of the star, but it is the strongest at the “propeller” regime of evolution.

We studied disk accretion to a star in the propeller regime by axisymmetric MHD simulations. In the propeller regime the centrifugal force at the external boundary of the rotating magnetosphere is larger than the gravitational force, so that accreting matter has a tendency to be flung away (e.g., [19] – [21]). We observed that there are two qualitatively different regimes: “weak” propeller regime (no outflows) or “strong” propeller regime (with outflows). In both cases the star strongly spins-down due to the interaction of the magnetosphere with the inner regions of the disk.

The weak propeller occurs when the transport coefficients in the disk (viscosity and diffusivity) are relatively small. Both viscosity and diffusivity were incorporated to the code and were considered in the simplified α -approach [22]. The weak propeller realizes at relatively small transport coefficients, $\alpha_{\text{vis}} < 0.2$ and $\alpha_{\text{dif}} < 0.2$. We observed that magnetic field lines inflate, forming a magnetic tower (see also [23]), that the closed magnetosphere expands in the radial direction, and matter accumulates near the magnetosphere and is blocked by the inflated magnetic flux from accretion. At some point, the accreting matter moves forward, forces magnetic field lines in the magnetosphere to reconnect and accretes to the star. Later, the magnetosphere expands again and the process repeats [24] (Figure 8). Such quasi-periodic accretion events have lower frequencies ν_{wp} at larger magnetic moments μ of the star and larger Ω_* . The typical frequency of the oscillations lies in the range $\nu_{wp} \approx 0.01\nu_*$ to $\nu_{wp} \approx 0.2\nu_*$ depending on parameters of the star and the disk.

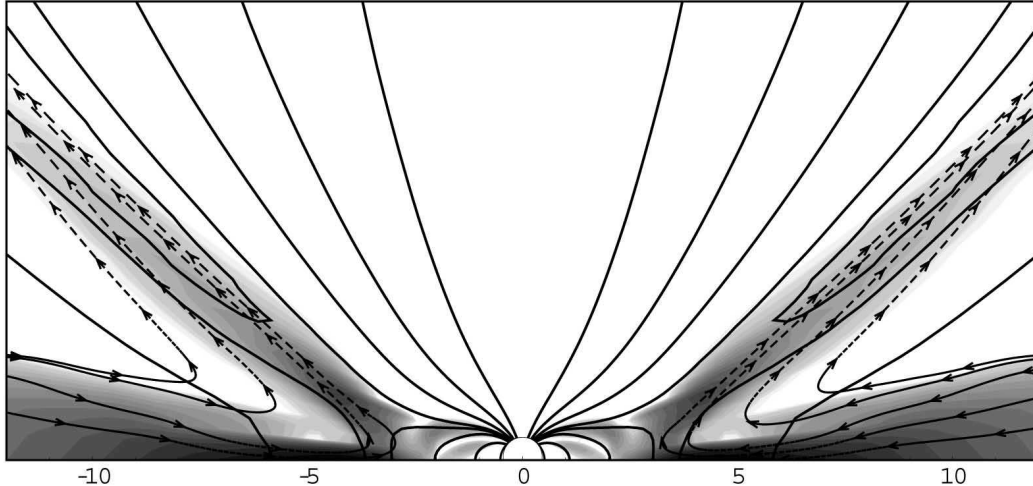


Fig. 9. Example of outflows at the “propeller” stage. Background and dashed lines show the angular momentum flux carried by matter. Solid lines are magnetic field lines.

The strong propeller (with outflows) was obtained when the viscosity and diffusivity in the disk were larger, $\alpha_{\text{vis}} \geq 0.2$ and $\alpha_{\text{dif}} \geq 0.2$. We observed that matter is ejected in the form of conical, wide-angle jets as a result of magneto-centrifugal forces [26],[27]. The process is quasi-periodic and we observed many periods of accretion and outflows. An example of outflows is shown in Figure 9. Important factors which led to propeller-driven outflows are the larger viscosity and diffusivity in the disk, which helped to transport momentum from the magnetosphere to the disk. Also, the enhanced viscosity helped the disk matter penetrate deeper into the rapidly rotating magnetosphere of the propeller. Both accretion and outflows occur quasi-periodically, which is connected with periods of (1) inward viscous accretion; (2) matter diffusion through the outer regions of magnetosphere and angular momentum transport from the magnetosphere to the disk; (3) accretion to the star and outburst to the jet; (4) outward motion of the disk (see also [23], [25]). The span of frequencies of quasi-periodic oscillations is similar to that in the weak propeller case, $\nu_{sp} \sim (0.01 - 0.2)\nu_*$. Figure 10 shows an example of the quasi-variable matter fluxes with a dominant low oscillation frequency $\nu_{sp} \approx (0.015 - 0.02)\nu_*$. We also noticed that at even higher viscosity, $\alpha_{\text{vis}} = 0.6$, the quasi-periodic oscillations became very ordered (see Figure 11). Their frequency was observed to drift slowly from $\nu_{sp} \approx 0.1\nu_*$ at the beginning of the simulation to $\nu_{sp} \approx 0.2\nu_*$ at the end of the simulation after > 1000 rotations of the star, because the disk moved closer to the star. Similar oscillations were observed in a test run with even higher viscosity [28].

We should note that the low-frequency variability is also observed in case of slowly rotating stars as a result of the restructuring of the magnetic field lines threading the inner regions of the disk (see Figure 1).

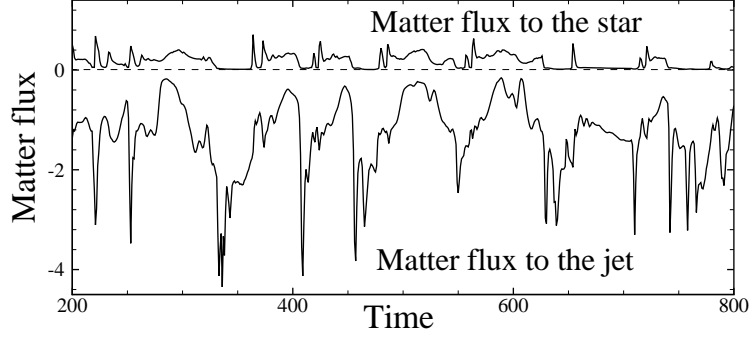


Fig. 10. Matter fluxes to the star and to the jet when $\alpha_{\text{vis}} = 0.3$ and $\alpha_{\text{dif}} = 0.2$. Time is measured in periods of Keplerian rotation at $r = 1$.

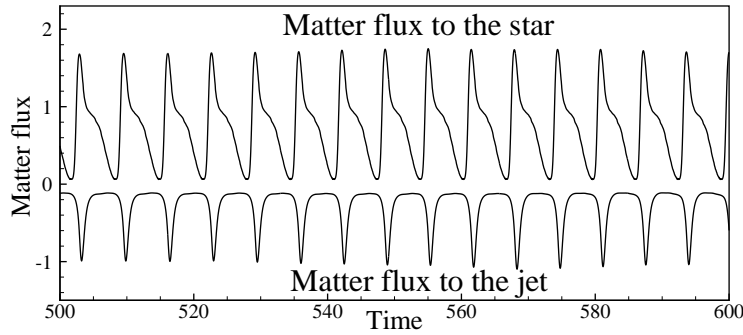


Fig. 11. Matter fluxes at $\alpha_{\text{vis}} = 0.6$ and $\alpha_{\text{dif}} = 0.2$. Time is measured in periods of Keplerian rotation at $r = 1$.

4 Conclusions

Analysis of the disk-magnetosphere interaction in axisymmetric and full 3D MHD simulations have shown that: (1) In the rotational equilibrium state, the ratio between frequencies of the inner disk and of the star is $\nu_m : \nu_* \approx (1.4 - 1.6)$ for magnetospheric radii $r_m \approx (3 - 6)R_*$. This ratio may possibly be larger for larger r_m ; (2) Non-axisymmetric features in the inner regions of the disk (typically, two-armed spirals, non-axisymmetry of the central density ring may lead to QPO oscillations with $\nu \sim 2\nu_m$; (3) At small misalignment angles Θ the funnels may precess, and thus may rotate faster/slower than the star; the frequency will vary between ν_* and ν_m or twice these values (depending on the number of spots); precession of funnels is expected during periods of non-stationary accretion; (4) In all cases the hot spots slightly change their position and shape which may lead to low-amplitude QPOs with frequency $\nu_{\text{spots}} \approx \nu_*$; (5) Low-frequency quasi-periodic oscillations were observed at the “propeller” stage, with dominant frequency in the range $\nu_p \leq (0.2 - 0.01)\nu_m$.

Acknowledgments. We are grateful to Prof. Ghosh for organizing such an excellent meeting and to Prof. F. Lamb and Prof. Poutanen for useful discussions. This work was supported in part by NASA grant NNG05GG77G,

and by NSF grants AST-0307817 and AST-0507760. AVK and GVU were partially supported by grant RFBR 06-02-16548.

References

- [1] Romanova, M.M., Ustyugova, G.V., Koldoba A.V., & Lovelace, R.V.E., Magnetohydrodynamic Simulations of Disk-Magnetized Star Interactions in the Quiescent Regime: Funnel Flows and Angular Momentum Transport, 2002, ApJ, 578, 420-438,
- [2] Pringle, J.E. & Rees, M.J., Accretion Disc Models for Compact X-Ray Sources, 1972, A&A, 21, 1P-9P.
- [3] Ghosh, P., & Lamb, F. K., Disk accretion by magnetic neutron stars, 1978, ApJ, 223, L83-L87.
- [4] Ghosh, P., & Lamb, F.K., Accretion by rotating magnetic neutron stars. III - Accretion torques and period changes in pulsating X-ray sources, 1979, ApJ, 234, 296-316.
- [5] Long, M., Romanova, M.M., & Lovelace, R.V.E., Locking of the Rotation of Disk-Accreting Magnetized Stars, 2005, ApJ, 634, 1214-1222.
- [6] van der Klis, M., Millisecond Oscillations in X-ray Binaries, 2000, Ann. Rev. Astron. Astrophys., 38, 717-760.
- [7] Wijnands, R., van der Klis, M., Homan, J., Chakrabarty, D., Markwardt, C. B., & Morgan, E. H., Quasi-periodic X-ray brightness fluctuations in an accreting millisecond pulsar, 2003, Nature, 424, 44-47.
- [8] Romanova, M.M., Ustyugova, G.V., Koldoba, A.V., & Lovelace, R.V.E., Three-dimensional Simulations of Disk Accretion to an Inclined Dipole. II. Hot Spots and Variability, 2004a, ApJ, 610, 920-932.
- [9] Lamb, F.K. 2006, these Proceedings
- [10] Koldoba, A.V., Romanova, M.M., Ustyugova, G.V., & Lovelace, R.V.E., Three-dimensional Magnetohydrodynamic Simulations of Accretion to an Inclined Rotator: The “Cubed Sphere” Method, 2002, ApJ, 576, L53-L56.
- [11] Romanova, M.M., Ustyugova, G.V., Koldoba, A.V., Wick, J.V., & Lovelace, R.V.E., Three-dimensional Simulations of Disk Accretion to an Inclined Dipole. I. Magnetospheric Flows at Different Θ , 2003, ApJ, 595, 1009-1031.
- [12] Kulkarni, A. & Romanova, M.M., Variability Profiles of Millisecond X-Ray Pulsars: Results of Pseudo-Newtonian Three-dimensional Magnetohydrodynamic Simulations, 2005, ApJ, 633, 349-357.
- [13] Pechenick, K.R., Ftaclas, C., & Cohen, J.M., Hot spots on neutron stars - The near-field gravitational lens, 1983, ApJ, 274, 846-857.

- [14] Poutanen, J., & Gierlinski, M., On the nature of the X-ray emission from the accreting millisecond pulsar SAX J1808.4-3658, 2003, MNRAS, 343, 1301-1311.
- [15] Beloborodov, A. M., Gravitational Bending of Light Near Compact Objects, 2002, ApJ, 566, L85-L88.
- [16] Alpar, M.A., & Shaham, J., Is GX5 - 1 a Millisecond Pulsar? 1985, Nature, 316, 239-241.
- [17] Lamb, F.K., Shibazaki, N., Alpar, M.A., & Shaham, J., Quasi-periodic Oscillations in Bright Galactic-bulge X-ray Sources, 1985, Nature, 317, 681-687.
- [18] Miller, M.C., Lamb, F.K., & Psaltis, D., Sonic-Point Model of Kilohertz Quasi-periodic Brightness Oscillations in Low-Mass X-Ray Binaries, 1998, ApJ, 508, 791-830.
- [19] Illarionov, A.F., & Sunyaev, R.A., Why the Number of Galactic X-ray Stars Is so Small?, 1975, A & A, 39, 185-195.
- [20] Lovelace, R.V.E., Romanova, M.M., & Bisnovatyi-Kogan, G.S., Magnetic Propeller Outflows, 1999, ApJ, 514, 368-372.
- [21] Eksi, K. Y., Hernquist, L., & Narayan, R., Where Are All the Fallback Disks? Constraints on Propeller Systems, 2005 ApJ, 623, L41-L44.
- [22] Shakura, N.I., & Sunyaev R.A. 1973, Black Holes in Binary Systems. Observational Appearance. A& A, 1973, 24, 337-355.
- [23] Kato, Y., Hayashi, M.R., & Matsumoto, R., Formation of Semirelativistic Jets from Magnetospheres of Accreting Neutron Stars: Injection of Hot Bubbles into a Magnetic Tower, 2004, ApJ, 600, 338-342.
- [24] Romanova, M.M., Ustyugova, G.V., Koldoba, A.V., & Lovelace, R.V.E., The Propeller Regime of Disk Accretion to a Rapidly Rotating Magnetized Star, 2004b, ApJ Lett., 616, L151-L154.
- [25] Goodson, A.P., Winglee, R. M., & Böhm, K.-H., Time-dependent Accretion by Magnetic Young Stellar Objects as a Launching Mechanism for Stellar Jets, 1997, ApJ, 489, 199-209.
- [26] Blandford, R.D., & Payne, D.G., Hydromagnetic flows from accretion discs and the production of radio jets, 1982, MNRAS, 199, 883-903.
- [27] Ustyugova, G.V., Koldoba, A.V., Romanova, M.M., & Lovelace, R.V.E., Magnetocentrifugally Driven Winds: Comparison of MHD Simulations with Theory, 1999, ApJ, 516, 221-235.
- [28] Romanova, M.M., Ustyugova, G.V., Koldoba, A.V., & Lovelace, R.V.E., Propeller-driven Outflows and Disk Oscillations, 2005, ApJ Lett., 635, L165-L168.